

Part One
Theory and Concepts

1

Accurate Dispersion-Corrected Density Functionals for General Chemistry Applications

Lars Goerigk and Stefan Grimme

1.1 Introduction

The aim of computational thermochemistry is to describe the energetic properties of chemical processes within an accuracy of 1 kcal mol^{-1} or less ($0.1\text{--}0.2 \text{ kcal mol}^{-1}$ for the relative energy of conformers). At the same time, the methods applied should not be too demanding in terms of necessary run times and hardware resources, which rules out highly accurate *ab initio* methods if larger, chemically relevant systems are to be considered. Whilst Kohn–Sham density functional theory [(KS-)DFT] offers an ideal solution to this dilemma [1, 2], the number of proposed exchange–correlation functionals is immense, and most of these suffer from severe problems. Very prominent examples are the self-interaction-error (SIE; also termed delocalization-error in many-electron systems) [3–6], and the lack of adequately describing long-range correlation effects, such as London-dispersion [7–10]. Moreover, the applicability of functionals to various problems is not broad but is rather specialized (see e.g., Ref. [11]) which, on occasion, makes their application very difficult for “non-experts.” In this chapter, two major contributions made by the authors’ laboratories will be reviewed, both of which should help in identifying the goal of developing accurate, robust, and broadly applicable methods. These two techniques are: (i) double-hybrid density functionals (DHDFs) [12]; and (ii) an atom-pair wise London-dispersion correction scheme (DFT-D, DFT-D3) [13–15].

Both approaches have been implemented into many quantum chemistry codes, have attracted worldwide interest, and have often been applied very successfully. The theoretical background of both approaches will be reviewed in the following sections, with particular attention focused on the very recently developed PWPB95 functional [16] and the newest version of the dispersion correction (DFT-D3) [15]. Three examples are then described demonstrating the benefits of both approaches. First, a large benchmark study is discussed in Section 1.3.1, with attention focused on the PWPB95 functional and DFT-D3. A mechanistic study of B2PLYP and the DFT-D scheme is then detailed (see Section 1.3.2), to help understand the details of a recently

reported reaction class. Finally, the description of excited states – and particularly of large chromophores – is shown to benefit from double-hybrid functionals (see Section 1.3.3).

1.2

Theoretical Background

1.2.1

Double-Hybrid Density Functionals

Double-hybrid density functionals are situated on the fifth rung in Perdew’s scheme of “Jacob’s ladder” [17], as they include virtual Kohn–Sham orbitals. Compared to hybrid-GGA functionals (fourth rung), where some part of the exchange functional is substituted by “exact” (HF) exchange, DHDFs additionally substitute some part of the correlation functional by mixing in a non-local perturbative correlation. This correlation part is basically obtained by a second-order Møller–Plesset (MP2)-type treatment based on KS orbitals and eigenvalues. The first DHDF according to this idea is the B2PLYP functional by Grimme [12]. The first step in a double-hybrid calculation is the generation of Kohn–Sham orbitals from the hybrid-GGA portion of the DHDF. In the case of B2PLYP, this portion is denoted as B2LYP.

$$E_{XC}^{B2LYP} = (1-a_X)E_X^{B88} + a_X E_X^{HF} + (1-a_C)E_C^{LYP} \quad (1.1)$$

This hybrid-GGA part contains Becke 1988 (B88) [18] exchange E_X^{B88} combined with non-local Fock-exchange E_X^{HF} and Lee–Yang–Parr (LYP) [19, 20] correlation E_C^{LYP} . The a_X and a_C are mixing parameters for the “exact” Fock-exchange and perturbative correlation, respectively. A second-order perturbation treatment (PT2), based on the KS-orbitals and eigenvalues resulting from the B2LYP calculation, is carried out yielding the correlation energy E_C^{PT2} that is scaled by the mixing parameter, a_C . Thus, the final form of the B2PLYP exchange correlation energy is given by:

$$E_{XC}^{B2PLYP} = E_{XC}^{B2(GP)-LYP} + a_C E_C^{PT2}. \quad (1.2)$$

The two mixing parameters were fitted to the heats of formation (HOFs) of the G2/97 set; these parameters are $a_X = 0.53$ and $a_C = 0.27$. Due to the perturbative contribution, B2PLYP formally scales with $\mathcal{O}(N^5)$, with N being the system size. However, if this step is evaluated using RI (density-fitting) schemes, the most time-consuming part is usually still the SCF and not the PT2 calculation.

Since B2PLYP, various other approaches have been reported, which are either modifications of B2PLYP [21–27] or are based on other (pure DFT-) exchange-correlation functionals [16, 28, 29]. These DHDFs usually differ in their amounts of Fock-exchange (between 50 and 82%). The impact of the Fock-exchange in a DHDF is depicted in Figure 1.1. Small amounts of E_X^{HF} within common hybrid-functionals are good for main group thermochemical properties; however, these functionals suffer more from the SIE which, for example, influences the result for barrier

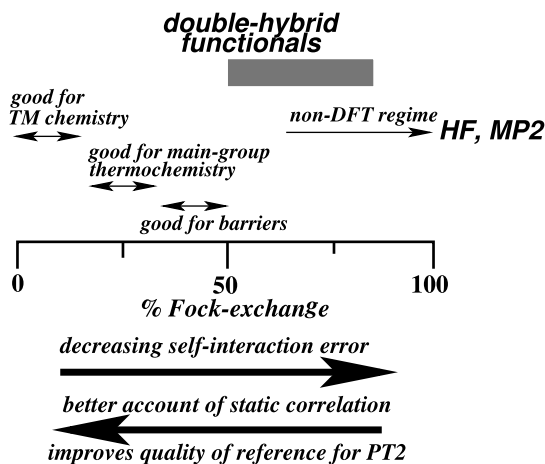


Figure 1.1 Effect of the amount of Fock-exchange in (double-)hybrid DFT calculations.

heights. Too-large amounts, on the other hand, render density functionals (DFs) unstable when treating transition metal compounds. Smaller amounts of Fock-exchange effectively mimic the effect of treating static electron correlation, which makes the perturbative correction more stable (than e.g., MP2) in electronically complicated situations. Thus, DHDFs are also applicable to many open-shell problems for which a Hartree–Fock reference would strongly suffer from spin-contamination.

As a compromise to treat main group and transition metal chemistry equally well, a new DHDF was recently developed by the present authors which just contains 50% of Fock-exchange [16]. This is dubbed PWPB95, and is based on the Perdew–Wang (PW) GGA-exchange [30] and the Becke95 (B95) meta-GGA-correlation [31] functionals (inspired by Zhao’s and Truhlar’s PW6B95 hybrid-meta-GGA [32]). It is, thus, the first DHDF with meta-GGA ingredients:

$$E_{XC}^{PWPB95} = (1-a_X)E_X^{PW} + a_X E_X^{HF} + (1-a_C)E_C^{B95} + a_C E_C^{OS-PT2}. \quad (1.3)$$

In contrast to other DHDFs, for which inherent functional parameters (e.g., β in B88) were not changed, PWPB95 is based on refitted PW and B95 parameters (three in the PW-exchange and two in the B95-correlation parts). Furthermore, PWPB95 includes a spin-opposite scaled second-order perturbative correlation contribution (OS-PT2) [33, 34]. Combined with an efficient Laplace transformation algorithm [35], this brings the formal scaling down from $\mathcal{O}(N^5)$ to $\mathcal{O}(N^4)$ with system size, which is the same as for conventional hybrid functionals.

The five inherent DFT parameters and the factor a_C were fitted on a fit set, covering various thermochemical energies (including noncovalent interactions). During the fitting procedure, the most recently developed empirical, atom-pairwise London-dispersion correction (DFT-D3) was applied [15]. The resulting non-local correlation scale factor is $a_C = 0.269$.

1.2.2

London-Dispersion-Corrected DFT

For more than a decade it has been recognized that commonly used DFs do not describe the long-range dispersion interactions correctly [7–10]. Originally, this was noted for rare gas dimers (e.g., as rediscovered in Ref. [36]), but later it was noticed also in base-pair stacking [37] or N_2 dimers [38]. During these early days some confusion arose because the problem is highly functional dependent. If equilibrium distances for common weakly bound complexes are mainly considered, some DFs (such as PW91 [30]) provide at least qualitatively correct interaction potentials, whilst for example, the popular BLYP or B3LYP [39, 40] approximations were found to be purely repulsive. Nowadays it is clear, that all semi-local DFs and conventional hybrid functionals (that include non-local Fock-exchange) asymptotically cannot provide the correct $-C_6/R^6$ dependence of the dispersion interaction energy on the interatomic(molecular) distance, R . This is different for intermediate distances, however, where the fragment electron densities overlap and semi-local DFs may yield bound states.

The various approaches that currently attempt to deal with that problem can be grouped into four classes (see Figure 1.2), which include: (i) non-local van der Waals functionals (vdW-DFs [41, 42]); (ii) “pure” (semi-local(hybrid)) DFs which are highly parameterized forms of standard meta-hybrid approximations (e.g., the M0XX family of functionals [43]); (iii) dispersion-correcting atom-centered one-electron potentials (1ePOT, called DCACP [44] or, in local variants LAP [45] or DCP [46]); and (iv) DFT-D methods (atom pair-wise sum over $-C_6 R^{-6}$ potentials [13–15, 47]). A recent review on London-dispersion-corrected DFT is available in Ref. [48].

In the following subsection, the DFT-D approach will be discussed in detail. This provides a dispersion energy E_{disp}^{DFT-D} , which can be added to the result of a standard DFT calculation. The general form for the dispersion energy is:

$$E_{disp}^{DFT-D} = -\frac{1}{2} \sum_{AB} \sum_{n=6,8,10,\dots} s_n \frac{C_n^{AB}}{R_{AB}^n} f_{damp}(R_{AB}). \quad (1.4)$$

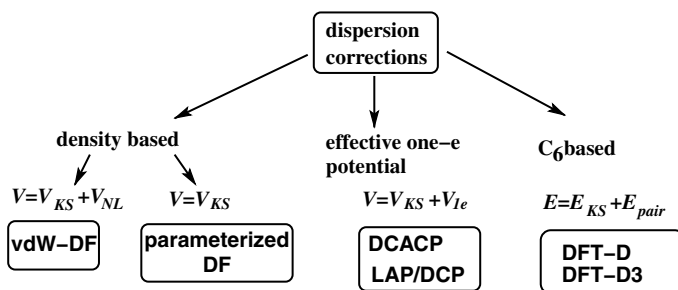


Figure 1.2 Overview of currently used dispersion corrections in DFT. E_{KS} and V_{KS} correspond to the bare Kohn–Sham total energies and potentials, respectively.

Here, the sum is over all atom pairs in the system, C_n^{AB} denotes the averaged (isotropic) n th-order dispersion coefficient (orders $n = 6, 8, 10, \dots$) for atom pair AB , and R_{AB} is their internuclear distance. Global (DF-dependent) scaling factors s_n are typically used to adjust the correction to the repulsive behavior of the chosen DF [13]. If this is done only for $n > 6$ (as in DFT-D3 [15]), asymptotic exactness is fulfilled when the C_6^{AB} are exact. It should be noted that the contribution of the higher-ranked multipole terms $n > 6$ is more short-ranged and rather strongly interferes with the (short-ranged) DF description of electron correlation. The higher C_n terms can be used to adapt the potential specifically to the chosen DF in this mid-range region.

In order to avoid near-singularities for small R and double-counting effects of correlation at intermediate distances, damping functions f_{damp} are used which determine the range of the dispersion correction (for a discussion of general damping functions, see Ref. [49]). If only noncovalent interactions are considered, the results are only weakly dependent on the specific choice of the function. A typical expression is [14]:

$$f_{damp}(R_{AB}) = \frac{1}{1 + e^{-\gamma(R_{AB}/s_{r,n}R_0^{AB}-1)}}, \quad (1.5)$$

where R_0^{AB} is a cut-off radius for atom pair AB , $s_{r,n}$ is a DF-dependent (global) scaling factor (as introduced in Ref. [47]), and γ is a global constant that determines the steepness of the functions for small R . For the cut-off radii, (averaged) empirical atomic vdW-radii are often used. Currently, the most widely used DFT-D method is the present authors' version (dating from 2006 [14]; now termed DFT-D2), which represents an update of DFT-D1 from 2004 [13]. The method has recently been refined regarding a higher accuracy, a broader range of applicability, and less empiricism (it is now termed DFT-D3 [15]). The main new ingredients are atom-pairwise specific dispersion coefficients and a new set of cut-off radii, both of which are computed from first principles. The coefficients for 8th-order dispersion terms are computed using established recursion relations. System (geometry) -dependent information is used for the first time in a DFT-D type approach by employing the new concept of fractional coordination numbers. This allows a distinction to be made, in a differentiable manner, between the different hybridization states of atoms in molecules which, in particular for the first two rows of the Periodic Table, have quite different dispersion coefficients. The method requires only an adjustment of two global parameters for each density functional, is asymptotically exact for a gas of weakly interacting neutral atoms, and easily allows the computation of atomic forces. Accurate dispersion coefficients and cut-off radii are available for all elements up to $Z = 94$. The revised DFT-D3 method can be used as a general tool for the computation of the dispersion energy in molecules and solids (see e.g., also Ref. [50, 51]) of any type with DFT and related (low-cost) electronic structure methods for a very recent modification of DFT-D3, also see Ref. [52]. Results for the DFT-D3 method are shown in Section 1.3.1 (the older DFT-D version is used in Section 1.3.2).

1.3

Examples

1.3.1

GMTKN30

In 2010, the present authors published the so-called GMTKN24 database, which is a collection of 24 previously reported or newly developed benchmark sets for general main group thermochemistry, kinetics, and noncovalent interactions [53]. Very recently, this was extended by six additional sets and dubbed GMTKN30 [16]. In total, the system comprises 1218 single point calculations and 841 data points (relative energies). The subsets of GMTKN30 can be divided into three major sections of: (i) basic properties (e.g., atomization energies, electron affinities, ionization potentials, proton affinities, SIE-related problems, barrier heights); (ii) various reaction energies (e.g., isomerizations, Diels–Alder reactions, ozonolyses, reactions involving alkaline metals); and (iii) noncovalent interactions (water clusters, relative energies between conformers, and inter- and intramolecular interactions). Reference values for all subsets are based on highly accurate theoretical or experimental data (for details, see the original reference [16]). GMTKN30 makes it possible to thoroughly evaluate existing methods, and also fosters the development of new DFs.

As handling the large number of statistical values for such a database can be unpractical, a so-called weighted total mean absolute deviation (WTMAD) was defined which combines all 30 mean absolute deviations (MADs) to one final number. For every subset, the size and “difficulty” is taken into account by a factor with which each MAD is scaled. Finally, the average is taken for these scaled MADs. Herein, this idea will be adopted and WTMADs calculated specifically for each of the three major sections of GMTKN30.

In the following, each of the three sections will first be discussed separately, after which an examination will be made of the complete benchmark set. Functionals of different rungs on Jacob’s Ladder will be investigated; these include BLYP and PBE [54] (GGAs), TPSS [55], and a recently re-fitted version oTPSS [53] (meta-GGAs), B3LYP and PW6B95 [32] (hybrids), B2PLYP, DSD-BLYP [26] and PWPB95 (DHDfFs).

In Figure 1.3, parts (a) to (c) show the WTMADs for the three sections of GMTKN30 for all functionals, with and without dispersion correction. All of these results are based on (aug-)def2-QZVP calculations, and were carried out with TURBOMOLE versions 5.9 and 6.0 [56–61]. Throughout the benchmark set, the benefit of including the dispersion correction can be clearly seen. For basic properties, which usually comprise rather small systems, DFT-D3 has the smallest impact, as expected, whereas for noncovalent interactions it has the largest impact. Furthermore, it is observed that a proper description of the dispersion effects is also very important for reaction energies. The WTMADs are lowered by 1 kcal mol^{-1} , or more. In all cases, there is a clear benefit from including non-local Fock-exchange, when passing from (meta-)GGAs to hybrids. An exception to this is the oTPSS functional, which yields similar results to B3LYP at less computational cost. Moreover, the results are improved when passing from hybrids to double-hybrids.

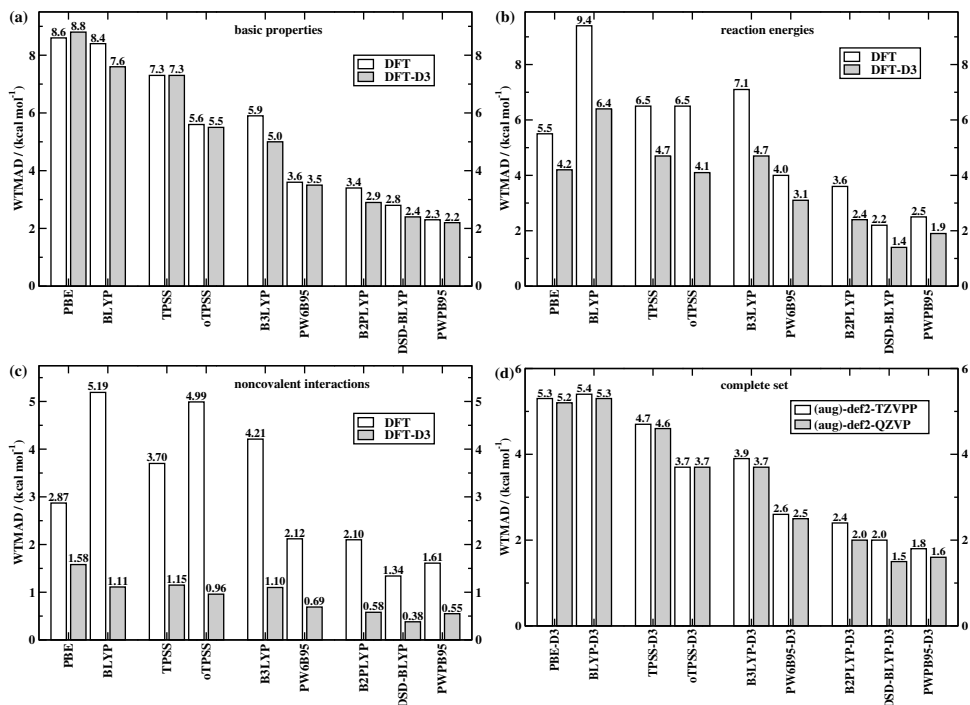


Figure 1.3 (a–c) Weighted total mean deviations (WTMADs) for the three major sections of GMTKN30 for various density functionals with (DFT-D3) and without dispersion correction (DFT). Results are based

on (aug)-def2-QZVP calculations; (d) WTMADs for the complete GMTKN30 database with dispersion correction for (aug)-def2-TZVPP and (aug)-def2-QZVP.

Figure 1.3(d) shows the WTMADs for the complete GMTKN30 set (only those results including the DFT-D3 correction are shown). Here, two different basis sets are compared with each other – one at triple- ζ level (usually used in applications) and one at the quadruple- ζ level. A comparison between both basis sets shows that (meta-)GGAs and hybrids are already at the Kohn–Sham limit with the large triple- ζ basis. The results differ much between both bases, with the meta-GGAs outperforming the GGAs and the hybrids outperforming the meta-GGAs. σ TPSS is again an exception, and is comparable to B3LYP. Based on the present authors’ experience, PW6B95 is the best general-purpose hybrid functional, with WTMADs of 2.6 and 2.5 kcal mol⁻¹, respectively. Due to the inclusion of a perturbative correction, double-hybrids are more basis set-dependent than hybrids. For example, B2PLYP-D3 is, with 2.4 kcal mol⁻¹ on the triple- ζ level, very close to PW6B95-D3 (2.6 kcal mol⁻¹), but improves more for the larger basis (2.0 kcal mol⁻¹). The only exception here is PWPB95-D3, which has a basis set-dependence similar to “conventional” functional; on the triple- ζ -level it is the best DHDF, whilst on the quadruple- ζ level it is the second best and very similar in many cases to DSD-BLYP-D3. A more thorough comparison with

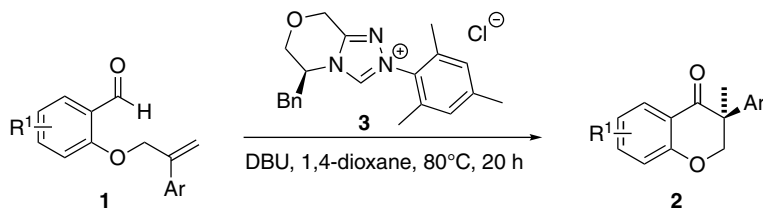


Figure 1.4 General reaction scheme and reaction conditions of the considered asymmetric hydroacylation. Several substituents R_1 were considered in the experimental work. The theoretical study was carried out for $R_1 = H$.

almost 50 functionals (including range-separated hybrids and Truhlar's M0X classes of functionals) was very recently undertaken at the authors' laboratories [62]. In addition, compared to these other more modern approaches, double-hybrids are the best functionals (they also turned out to be more accurate than various MP2 methods at the same computational cost). Results for 3d-transition metals have also shown much promise [16], indicating that PWPB95-D3 is the best DHDF.

1.3.2

A Mechanistic Study with B2PLYP-D

A recent example, in which a DHDF was applied to a practically relevant problem, was reported by Piel *et al.*, who presented an asymmetric hydroacylation reaction of unactivated olefins (Figure 1.4) [63]. The reaction is aided by the chiral N-heterocyclic carbene (NHC) **3** as a catalyst. First, an intermediate 1_{int} is formed, which is the result of a nucleophilic attack of the NHC at the carbonyl group of **1**. The following step is a hydrogen-transfer between the hydroxy group and the terminal carbon atom of the carbon-carbon double bond to yield the second intermediate 2_{int} , which then reacts to **2**. To better understand this transfer reaction, a theoretical study was carried out whereby two different reaction pathways were calculated, in which the stereochemistry of the reaction was investigated. Consequently, two intermediates are considered, which were formed by the NHC attacking either the Re- or the Si-side of the electrophilic carbonyl-C-atom.

BP86-D [64, 65]/TZVP [66] geometry optimizations and subsequent B2PLYP-D/TZVPP single-point calculations of the intermediates and the transition states were carried out. In both cases, the transition state structures (2_{TS1} and 2_{TS2}) are characterized by a stacked arrangement of the aromatic moieties, which shows the importance of including a dispersion correction in the treatment (Figure 1.5). Figure 1.5 also shows the relative energies of the transition states and product intermediates compared to the substrate intermediates. Qualitatively, BP86-D and B2PLYP-D give the same result – that is, reaction pathway 1 is favored. The transition state of pathway 2 lies energetically higher, due to steric hindrance of the benzyl group of the catalyst, and this in turn explains the high enantioselectivity of this reaction. The results for both functionals differed quantitatively, however, with the BP86-D barriers for both pathways being very low because of the SIE (4.0 and 8.7 kcal mol⁻¹). B2PLYP-D gives higher barriers (10.0 and 15.4 kcal mol⁻¹), which is in much better

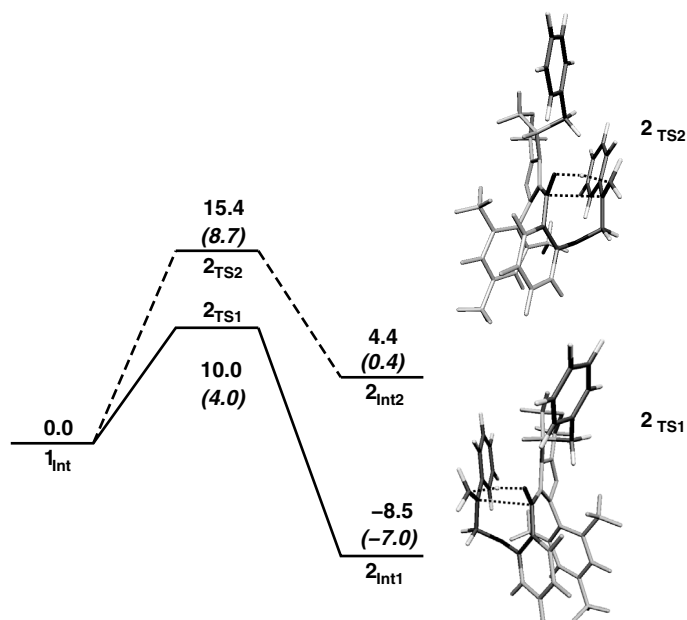


Figure 1.5 Calculated relative energies for the two reaction pathways leading to two diastereomeric transition states. Calculations are based on the B2PLYP-D/TZVPP and BP86-

D/TZVP (values in parentheses) levels of theory. The structures on the right-hand side show the two transition states. The dotted lines indicate the proton transfer.

agreement with the experiment, which must be carried out at 80 °C in order to obtain reasonable reaction rates. Thus, the application of a DHDF was crucial for a correct understanding of the reaction mechanism.

1.3.3

Double-Hybrids for Excited States

The accurate description of the electronically excited states of large organic dyes represents a challenging task for modern quantum chemistry. One current aim in this field of research is to correctly predict absolute excitation energies within an error of ± 0.1 eV (“chemical accuracy”) for large chromophores (20–30, or more, non-hydrogen atoms). Moreover, because the human eye can resolve frequency differences as small as 0.01–0.02 eV, it would be desirable to predict different chromophores or substituent effects on a similar relative scale of accuracy. Generally, on the “wish list” here are methods that are accurate, broadly applicable and do not contain systematic corrections, and which have to be considered by the user (e.g., the application of red- or blue-shifts dependent on systematic, methodological errors).

In 2007, Grimme and Neese suggested a way to achieve this aim by treating excited states with double-hybrid functionals [67]. The resultant TD-DHDF theory proved to

be excellent for the calculation of circular dichroism spectra [68] and a general benchmark of small molecules [69]. Here, the results are presented for the B2PLYP and B2GPPLYP [22] methods, where the latter differs from the former simply by the amounts of mixed-in Fock-exchange and perturbative correlation. In a TD-DHDF calculation, the hybrid-GGA part with 53% (B2PLYP) and 65% of Fock-exchange (B2GPPLYP) is used for a standard TD-DFT treatment. Subsequently, by using the resultant excitation amplitudes and the orbitals of the ground-state Kohn–Sham determinant, a standard CIS(D)-type calculation can be carried out. The resulting perturbative energy correction is then scaled by the (ground-state) correlation energy scaling factors of 0.27 (B2PLYP) or 0.36 (B2GPPLYP), respectively, and added to the TD-DFT excitation energy. At this point, the performance of double-hybrids for large organic chromophores will be reviewed and discussed. For such hybrids, conventional TD-DFT methods may fail, while *ab initio* methods are usually not feasible. Recently, a benchmark set of 12 large organic dyes was reported (see Figure 1.6) [69, 70], which were composed of various chromophores, sometimes including heteroatoms. Of these species, two were positively charged, and one system had a very prominent charge-transfer excitation. Only the lowest-lying, most bright $\pi \rightarrow \pi^*$ vertical transitions in the gas phase were considered. The reference values were based on experimental 0-0-transitions in solution that were back-corrected for vibrational and solvent effects. The accuracy of these data was estimated at ± 0.1 eV. The mean deviations (MDs) and mean absolute deviations (MADs) from these reference data for various TD-DFT and *ab initio* methods are shown in Figure 1.7.

Functionals such as BLYP and B3LYP yield large systematic errors, as shown by the strong underestimation of excitation energies (MDs of -0.49 and -0.22 eV) and the relatively large MAD-values (0.51 and 0.31 eV). With an increasing amount of Fock-exchange mixing – and thus a reduced self-interaction error as likely source – PBE38 (with 37.5% of Fock-exchange) performed better and showed an MD of 0.04 eV and an MAD of only 0.19 eV. Another possible approach to improving the results is the application of range-separated functionals, as demonstrated here with CAM-B3LYP (MAD of 0.18 eV). The double-hybrid B2PLYP is also very promising (MD = -0.11 eV; MAD = 0.20 eV), while B2GPPLYP is the most robust functional and yields the smallest MD (-0.01 eV) and MAD (0.16 eV). B2GPPLYP also competes with the *ab initio* approaches SCS-CIS(D), SCS-CC2 and CC2 (which is often regarded as “gold standard” for large chromophores). Although chemical accuracy on average (0.1 eV error) has not yet been reached, double-hybrid functionals are clearly pointing into the right direction, and their further development appears very promising. In particular, B2GPPLYP seems ideal for treating excited states.

1.4 Summary and Conclusions

An overview has been provided of two recent advances in DFT, namely double-hybrid DFT and the empirical London-dispersion-correction schemes, DFT-D/DFT-D3. While discussing three examples, it was shown in a large benchmark study that

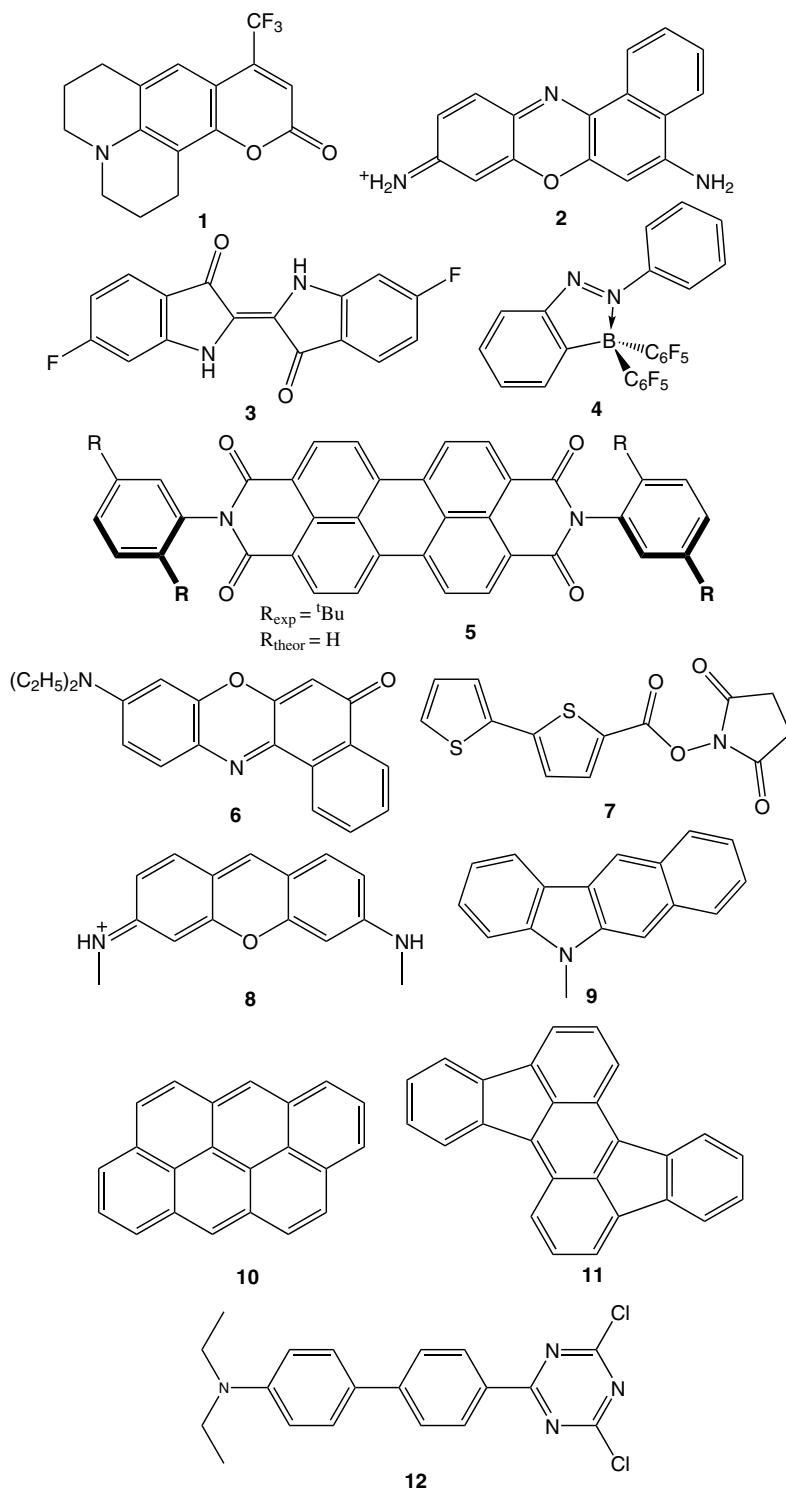


Figure 1.6 Chemical structures of the dye benchmark set.

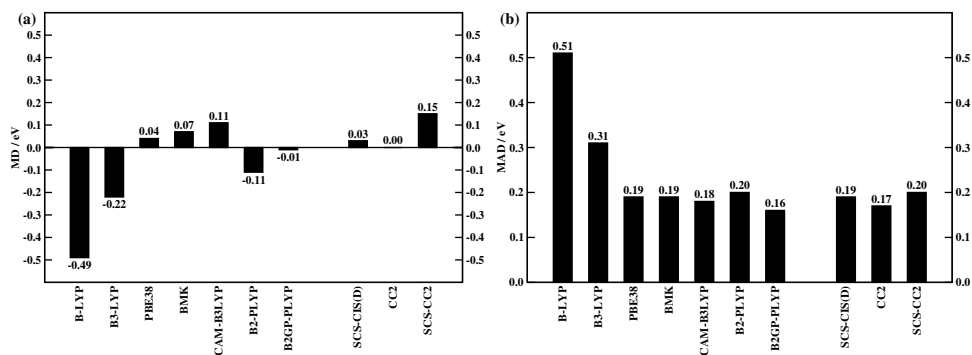


Figure 1.7 (a) Mean deviations (MD) and (b) mean absolute deviations (MAD) of various TD-DFT and *ab initio* methods for the dye benchmark set.

dispersion effects are important not only for an adequate description of noncovalent interactions, but also for obtaining accurate reaction energies. Double-hybrids, and in particular the new PWPB95 functional, were shown to be the most robust and best functionals for main group thermochemistry, kinetics, and noncovalent interactions. The second example reviewed the application of B2PLYP-D to a chemically relevant problem. Here, it was found that B2PLYP was necessary for obtaining reasonable reaction barriers, and the DFT-D correction scheme was crucial for properly describing intramolecular dispersion effects in geometry optimizations. Finally, the double-hybrids were shown to be useful not only for electronic ground state-related problems, but also for excited states. Indeed, in a test set of large dye chromophores they were able to compete even with *ab initio* methods. In general, the use of double-hybrids and the DFT-D scheme for obtaining accurate and reliable results, is strongly recommended.

Acknowledgments

Part of these studies were conducted within the framework of the SFB 858, DFG “Synergetische Effekte in der Chemie – Von der Additivität zur Kooperativität”. L. G. was supported by a scholarship from the “Fonds der Chemischen Industrie.” The authors also wish to thank C. Mück-Lichtenfeld for technical assistance.

References

- Hohenberg, P. and Kohn, W. (1964) *Phys. Rev. B*, **136**, 864–871.
- Kohn, W. and Sham, L.J. (1965) *Phys. Rev.*, **140**, A1133–A1138.
- Zhang, Y. and Yang, W. (1998) *J. Chem. Phys.*, **109**, 2604–2608.
- Gritsenko, O., Ensing, B., Schipper, P.R.T., and Baerends, E.J. (2000) *J. Phys. Chem. A*, **104**, 8558–8565.
- Ruzsinszky, A., Perdew, J.P., Csonka, G.I., Vydrov, O.A., and Scuseria, G.E. (2007) *J. Chem. Phys.*, **126**, 104102.

- 6 Mori-Sanchez, P., Cohen, A.J., and Yang, W. (2006) *J. Chem. Phys.*, **125**, 201102.
- 7 Kristyán, S. and Pulay, P. (1994) *Chem. Phys. Lett.*, **229**, 175–180.
- 8 Hobza, P., Sponer, J., and Reschel, T. (1995) *J. Comput. Chem.*, **16**, 1315–1325.
- 9 Pérez-Jordá, J.M. and Becke, A.D. (1995) *Chem. Phys. Lett.*, **233**, 134–137.
- 10 Pérez-Jordá, J.M., San-Fabián, E., and Pérez-Jiménez, A.J. (1999) *J. Chem. Phys.*, **110**, 1916–1920.
- 11 Rappoport, D., Crawford, N.R.M., Furche, F., and Burke, K. (2009) Approximate density functionals: which should I choose? in *Computational Inorganic and Bioinorganic Chemistry* (eds E.I. Solomon, R.A. Scott, and R.B. King), Wiley-VCH, New York, pp. 159–172.
- 12 Grimme, S. (2006) *J. Chem. Phys.*, **124**, 034108.
- 13 Grimme, S. (2004) *J. Comput. Chem.*, **25**, 1463–1473.
- 14 Grimme, S. (2006) *J. Comput. Chem.*, **27**, 1787–1799.
- 15 Grimme, S., Antony, J., Ehrlich, S., and Krieg, H. (2010) *J. Chem. Phys.*, **132**, 154104.
- 16 Goerigk, L. and Grimme, S. (2011) *J. Chem. Theory Comput.*, **7**, 291–309.
- 17 Perdew, J.P., Ruzsinszky, A., Tao, J., Staroverov, V.N., Scuseria, G.E., and Csonka, G. (2005) *J. Chem. Phys.*, **123**, 62201.
- 18 Becke, A.D. (1988) *Phys. Rev. A*, **38**, 3098–3100.
- 19 Lee, C., Yang, W., and Parr, R.G. (1988) *Phys. Rev. B*, **37**, 785–789.
- 20 Miehlich, B., Savin, A., Stoll, H., and Preuss, H. (1989) *Chem. Phys. Lett.*, **157**, 200–206.
- 21 Tarnopolsky, A., Karton, A., Sertchook, R., Vuzman, D., and Martin, J.M.L. (2008) *J. Phys. Chem. A*, **112**, 3–8.
- 22 Karton, A., Tarnopolsky, A., Lamère, J.F., Schatz, G.C., and Martin, J.M.L. (2008) *J. Phys. Chem. A*, **112**, 12868–12886.
- 23 Sancho-García, J.C. and Pérez-Jiménez, A.J. (2009) *J. Chem. Phys.*, **131**, 084108.
- 24 Benighaus, T., DiStasio, R.A., Jr., Chai, J.-D., and Head-Gordon, M. (2008) *J. Phys. Chem. A*, **112**, 2702–2712.
- 25 Graham, D.C., Menon, A.S., Goerigk, L., Grimme, S., and Radom, L. (2009) *J. Phys. Chem. A*, **113**, 9861–9873.
- 26 Kozuch, S., Gruzman, D., and Martin, J.M.L. (2010) *J. Phys. Chem. C*, **114**, 20801–20808.
- 27 Zhang, Y., Xu, X., and Goddard, W.A. III (2009) *Proc. Natl Acad. Sci. USA*, **106**, 4963–4968.
- 28 Grimme, S. and Schwabe, T. (2006) *Phys. Chem. Chem. Phys.*, **8**, 4398–4401.
- 29 Chai, J.-D. and Head-Gordon, M. (2009) *J. Chem. Phys.*, **131**, 174105.
- 30 Perdew, J.P. (1991) in Proceedings of the 21st Annual International Symposium on the Electronic Structure of Solids (eds P. Ziesche and H. Eschrig), Akademie Verlag, Berlin, p. 11.
- 31 Becke, A.D. (1996) *J. Chem. Phys.*, **104**, 1040–1046.
- 32 Zhao, Y. and Truhlar, D.G. (2005) *J. Phys. Chem. A*, **109**, 5656–5667.
- 33 Grimme, S. (2003) *J. Chem. Phys.*, **118**, 9095–9102.
- 34 Jung, Y., Lochan, R.C., Dutoi, A.D., and Head-Gordon, M. (2004) *J. Chem. Phys.*, **121**, 9793–9802.
- 35 Almlöf, J. (1991) *Chem. Phys. Lett.*, **181**, 319–320.
- 36 Kurita, N. and Sekino, H. (2001) *Chem. Phys. Lett.*, **348**, 139–146.
- 37 Sponer, J., Leszczynski, J., and Hobza, P. (1996) *J. Comput. Chem.*, **17**, 841–850.
- 38 Couronne, O. and Ellinger, Y. (1999) *Chem. Phys. Lett.*, **306**, 71–77.
- 39 Becke, A.D. (1993) *J. Chem. Phys.*, **98**, 5648–5652.
- 40 Stephens, P.J., Devlin, F.J., Chabalowski, C.F., and Frisch, M.J. (1994) *J. Phys. Chem.*, **98**, 11623–11627.
- 41 Dion, M., Rydberg, H., Schröder, E., Langreth, D.C., and Lundqvist, B.I. (2004) *Phys. Rev. Lett.*, **92**, 246401.
- 42 Lee, K., Murray, E.D., Kong, L., Lundqvist, B.I., and Langreth, D.C. (2010) *Phys. Rev. B*, **82**, 081101.
- 43 Zhao, Y. and Truhlar, D.G. (2008) *Acc. Chem. Res.*, **41**, 157–167.

- 44 von Lilienfeld, O.A., Tavernelli, I., Röthlisberger, U., and Sebastiani, D. (2004) *Phys. Rev. Lett.*, **93**, 153004.
- 45 Sun, Y.Y., Kim, Y.-H., Lee, K., and Zhang, S.B. (2008) *J. Chem. Phys.*, **129**, 154102.
- 46 Johnson, E.R., Mackie, I.D., and DiLabio, G.A. (2009) *J. Phys. Org. Chem.*, **22**, 1127–1135.
- 47 Jurečka, P., Cerny, J., Hobza, P., and Salahub, D.R. (2007) *J. Comput. Chem.*, **28**, 555–569.
- 48 Grimme, S. (2011) Density functional theory with London dispersion corrections, in *Wiley Interdisciplinary Reviews: Computational Molecular Science (WIREs:CMS)*, John Wiley & Sons, Hoboken, NJ.
- 49 Liu, Y. and Goddard, W.A. III (2009) *Mater. Trans.*, **50**, 1664–1670.
- 50 Moellmann, J. and Grimme, S. (2010) *Phys. Chem. Chem. Phys.*, **12**, 8500–8504.
- 51 Yousaf, K.E. and Brothers, E.N. (2010) *J. Chem. Theory Comput.*, **6**, 864–872.
- 52 Grimme, S., Ehrlich, S., and Goerigk L. (2011) *J. Comput. Chem.*, **32**, 1456–1465.
- 53 Goerigk, L. and Grimme, S. (2010) *J. Chem. Theory Comput.*, **6**, 107–126.
- 54 Perdew, J.P., Burke, K., and Ernzerhof, M. (1996) *Phys. Rev. Lett.*, **77**, 3865–3868.
- 55 Tao, J., Perdew, J.P., Staroverov, V.N., and Scuseria, G.E. (2003) *Phys. Rev. Lett.*, **91**, 146401.
- 56 Weigend, F. and Ahlrichs, R. (2005) *Phys. Chem. Chem. Phys.*, **7**, 3297–3305.
- 57 Kendall, R.A., Dunning, T.H., and Harrison, R.J. (1992) *J. Chem. Phys.*, **96**, 6796–6806.
- 58 Ahlrichs, R. et al. TURBOMOLE: Universität Karlsruhe 2008 and 2009. Available at: <http://www.turbomole.com> (accessed 9 November 2010).
- 59 Ahlrichs, R., Bär, M., Häser, M., Horn, H., and Kölmel, C. (1989) *Chem. Phys. Lett.*, **162**, 165–169.
- 60 Eichkorn, K., Treutler, O., Öhm, H., Häser, M., and Ahlrichs, R. (1995) *Chem. Phys. Lett.*, **240**, 283–289.
- 61 Hättig, C. and Weigend, F. (2000) *J. Chem. Phys.*, **113**, 5154–5161.
- 62 Goerigk, L. and Grimme, S. (2011) *Phys. Chem. Chem. Phys.*, **13**, 6670–6688.
- 63 Piel, I., Steinmetz, M., Hirano, K., Frölich, R., Grimme, S., and Glorius, F. (2011) *Angew. Chem. Int. Ed.*, **50**, 4983–4987.
- 64 Perdew, J.P. (1986) *Phys. Rev. B*, **33**, 8822–8824.
- 65 Perdew, J.P. (1986) *Phys. Rev. B*, **34**, 7406.
- 66 Schäfer, A., Huber, C., and Ahlrichs, R. (1994) *J. Chem. Phys.*, **100**, 5829–5835.
- 67 Grimme, S. and Neese, F. (2007) *J. Chem. Phys.*, **127**, 154116.
- 68 Goerigk, L. and Grimme, S. (2009) *J. Phys. Chem. A*, **113**, 767–776.
- 69 Goerigk, L., Moellmann, J., and Grimme, S. (2009) *Phys. Chem. Chem. Phys.*, **11**, 4611–4620.
- 70 Goerigk, L. and Grimme, S. (2010) *J. Chem. Phys.*, **132**, 184103.